Available online at www.sciencedirect.com
SCIENCE DIRECT®
Surface Science 598 (2005) L339–L346
SURFACE SCIENCE
www.elsevier.com/locate/susc

Surface Science Letters

# Global structural optimization of Si magic clusters on the Si(1 1 1) 7 × 7 surface

Feng-Chuan Chuang *, Bei Liu, Cai-Zhuang Wang, Tzu-Liang Chan, Kai-Ming Ho

*Ames Laboratory, US Department of Energy and Department of Physics and Astronomy, Iowa State University, Ames, IA 50011, USA*

Received 13 March 2005; accepted for publication 16 September 2005
Available online 21 October 2005

**Abstract**

We performed global structural optimization using a genetic algorithm in combination with tight-binding and first-principles calculations to study the structures of the magic clusters on the Si(1 1 1) 7 × 7 surface. Our calculations show that the magic cluster observed in scanning tunneling microscopy (STM) experiment [I.S. Hwang, M.S. Ho, T.T. Tsong, Phys. Rev. Lett. 83 (1999) 120] consists of eight Si atoms on the faulted half of the Si(1 1 1) 7 × 7 surface. Simulated STM images of our Si magic cluster exhibit a ring-like feature similar to STM experiments.
© 2005 Elsevier B.V. All rights reserved.

*Keywords:* Clusters; Self-assembly; Molecular dynamics; Density functional calculations; Scanning tunneling microscopy; Surface energy; Silicon; Low index single crystal surfaces

Magic clusters and ordered arrays of magic-sized structures on semiconductor surfaces [1–4] may play an important role in the fabrication of surface nanostructures with uniform size and shape distribution. Formation of Si magic clusters on the Si(1 1 1) 7 × 7 surface has been studied by Hwang et al. [1] using scanning tunneling microscopy (STM). These magic clusters are energetically stable entities on the substrate and are able to diffuse as a whole. It has been showed that Si magic clusters on the Si(1 1 1) 7 × 7 surface are the fundamental units in mass transport phenomena, step fluctuations, detachment and attachment of Si atoms at step edges, and epitaxial growth [1]. More recently, ordered arrays of nanoclusters formed upon deposition of Al, In, and Ga on the

* Corresponding author. Tel.: +1 5152946934; fax: +1 5152940689.
*E-mail addresses:* fchuang@iastate.edu (F.-C. Chuang), wangcz@ameslab.gov (C.-Z. Wang).

0039-6028/$ - see front matter © 2005 Elsevier B.V. All rights reserved.
doi:10.1016/j.susc.2005.09.025

Si(1 1 1) $7\times7$ surface have also been observed experimentally using STM [2–4].

While STM studies give valuable information about the overall shape and the size of the magic clusters on the Si(1 1 1) $7\times7$ surface, the images from STM cannot provide exact determination of the detailed atomic structure of the magic clusters. A comprehensive understanding of the structural and dynamical properties of the magic clusters on the surfaces would be very important for precise manipulation of nanostructures assembly on semiconductor substrate and for studying the properties of these assembled nanostructures.

In this paper, we focus on determining the structures of the Si magic clusters on the Si(1 1 1) $7\times7$ surface as a first step towards understanding their atomic structures, electronic properties, and future applications. Global structural optimization is developed and performed using genetic algorithm (GA) coupled with the environment-dependent Si tight-binding (TB) potential [5]. The low energy candidates selected from the GA optimizations were further relaxed using first-principles total energy calculations. Simulated STM images were calculated to compare with experimental observations.

The STM studies by Hwang et al. showed that Si magic clusters appear on the faulted half of the Si(1 1 1) $7\times7$ unit cell, and are approximately 1.5 Å higher than the Si adatoms of the Si(1 1 1) $7\times7$ surface [1]. The mirror symmetry of the $(7\times7)$ reconstruction along the $[\bar{1}\,\bar{1}\,2]$ direction is broken due to the presence of the cluster. The empty state STM image shows six or three protrusions of nearly equal brightness forming a ring-like structure [1]. The spacing between adjacent protrusions is much larger than the length of the Si–Si bond, indicating that the cluster probably contains more than six Si atoms. The size of the magic cluster is estimated to be between 9 and 15 Si atoms by Hwang et al. Dynamical studies show that these magic clusters diffuse as a unit and are still observable up to a temperature of 500 °C. While the magic clusters diffuse on the surface, the detachment of those clusters leave the surface intact. This experimental information is very useful for guiding the design of our atomic structure search strategy as described below.

The genetic algorithm (GA) has been used successfully in global structural optimization for isolated medium-sized silicon clusters [6,7]. Very recently, we have also successfully applied the genetic algorithm to study the reconstructions of high-index silicon surfaces [8,9]. We note that the total number of atoms involved in a Si(1 1 1) $7\times7$ substrate is too large for performing such global minimum search using tight-binding potential. Obviously, the total number of the atoms involved in the GA operations needs to be reduced. Since the magic clusters are found to be located on one half of the $7\times7$ unit cell, our GA optimization is performed only on a half unit cell of the $7\times7$ reconstruction together with the dimers at the boundary between the faulted and the unfaulted halves of the $(7\times7)$ reconstruction as shown in Fig. 1. We also note that the bonding between the magic cluster and the substrate involves mostly the top substrate atoms since diffu-

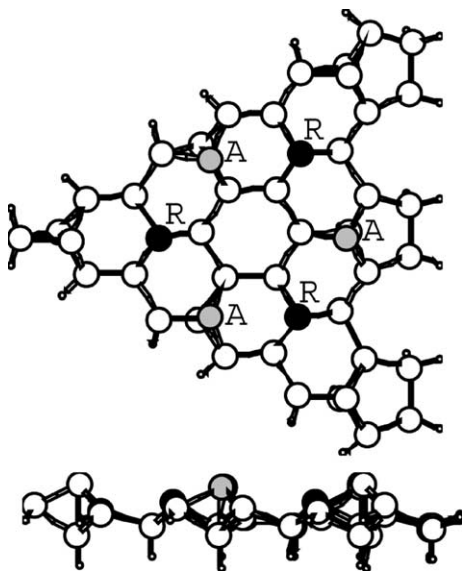


Fig. 1. The top view (upper) and the side view (lower) of the half unit cell Si(1 1 1) $7\times7$ substrate used in our genetic algorithm. The three adatoms (labeled with A) and the three rest atoms (labeled with R) involved in the GA mating process are those in grey and black, respectively, whereas the atoms which are not involved in the GA operation are shown in white. Big white circles are the Si atoms, whereas the small circles are the H atoms. The Si dangling bonds at the edges and at the bottom of the unit cell are passivated with hydrogen.

sion of the magic cluster leaves the surface reconstruction intact. Therefore, only one Si bilayer is used to model the substrate in order to further reduce the number of atoms involved in the GA optimization. The bottom layer of the slab and the Si dangling bonds at the edge of the unit cell are passivated by hydrogen atoms. The final modeling substrate is shown in Fig. 1.

Once the substrate is chosen, the procedures of our genetic algorithm are as follows. We generate ten geometries as initial population ($p = 10$) by randomly placing a specific number of Si atoms $n$ on the half unit cell and then relaxing the structure to a local minimum. The relaxation is done using tight-binding potential with the steepest descent method. In each subsequent generation, four distinct geometries are randomly picked from the population pool. Then twelve new geometries are generated from the four parents through the mating operation described below. These children geometries are then relaxed to their nearest local minima. The population of ten geometries in the pool is updated if any child geometry has different structure and lower energy than any of those in the present population pool. The genetic algorithm was implemented up to 400 generations.

The mating operation produces a child geometry C from the two given parent geometries A and B as follows. For each of the parent geometry, the atoms in the cluster along with three rest atoms and three adatoms (the dark and grey atoms in Fig. 1) on a half unit cell substrate are chosen to be mated. The centers of mass of these chosen atoms in both geometries are then calculated and both parents are cut through the centers of mass with randomly chosen parallel planes. The child geometry C is created by assembling the right half of the chosen atoms in the parent A and the left half of the chosen atoms in the parent B. The resultant atomic configuration of this child C is placed back on the substrate which has three rest atoms and three adatoms removed as illustrated in Fig. 1. During the mating process, the number of atoms in the resultant child C is forced to be the same as that in its parents.

We note that the energy calculations using a one-bilayer substrate cannot differentiate between faulted half and unfaulted half of the Si(1 1 1) $7 \times 7$ substrate. Therefore, the candidate geometries obtained by our genetic algorithm described above are further optimized using TBMD by augmenting the structures with a two-bilayer full Si $7 \times 7$ substrate. The bottom layer of the substrate is passivated by H, and this two-bilayer full Si $7 \times 7$ substrate contains 200 Si atoms and 49 H atoms with a periodic boundary condition parallel to the surface. Two individual optimizations of each structure are done by putting the cluster on either the faulted half or the unfaulted half of the substrate. Finally, the best geometries obtained from genetic algorithm and TBMD optimizations are further studied by first-principles total energy calculations using the same full Si $7 \times 7$ two-bilayer substrate containing 200 Si atoms and 49 H atoms. First-principles calculations in this work have been done using the PWscf package [10], which is based on density functional theory [11] under local density approximations and uses pseudopotential and plane wave basis. The Ceperley–Alder functional [12] parameterized by Perdew and Zunger [13] is used for the exchange-correlation energy functional. The kinetic energy cutoff is set to be 12 $Ry$ and $\Gamma$-point is used in the Brillouin zone sum. A vacuum layer of 12 Å is used in the calculations. Moreover, the structures are optimized until the forces are less than 0.025 eV/Å.

We have performed global structural optimizations for Si clusters on Si(1 1 1) $7 \times 7$ for sizes ranging from $n = 6$ to $n = 14$. The lowest energy structure of each size is showed in Fig. 2 where only the faulted half of the $7 \times 7$ unit cell is shown for clarity. In all structures, one of the substrate adatoms is found to be incorporated into the Si cluster. This incorporation will leave three back-bond atoms unbonded and the Si cluster will subsequently anchor itself to these back-bond atoms. This structural feature justifies the necessity of including the three adatoms and the three rest atoms of the substrate in our GA mating operation. For $n = 6$, the structure obtained by placing six Si atoms at the bright spots as indicated in the STM experiment [1] is not stable according to our first-principles calculations. Instead, our genetic algorithm for $n = 6$ found that a six-member ring with an extra Si atom at the center is the lowest energy structure as shown in Fig. 2(a). The

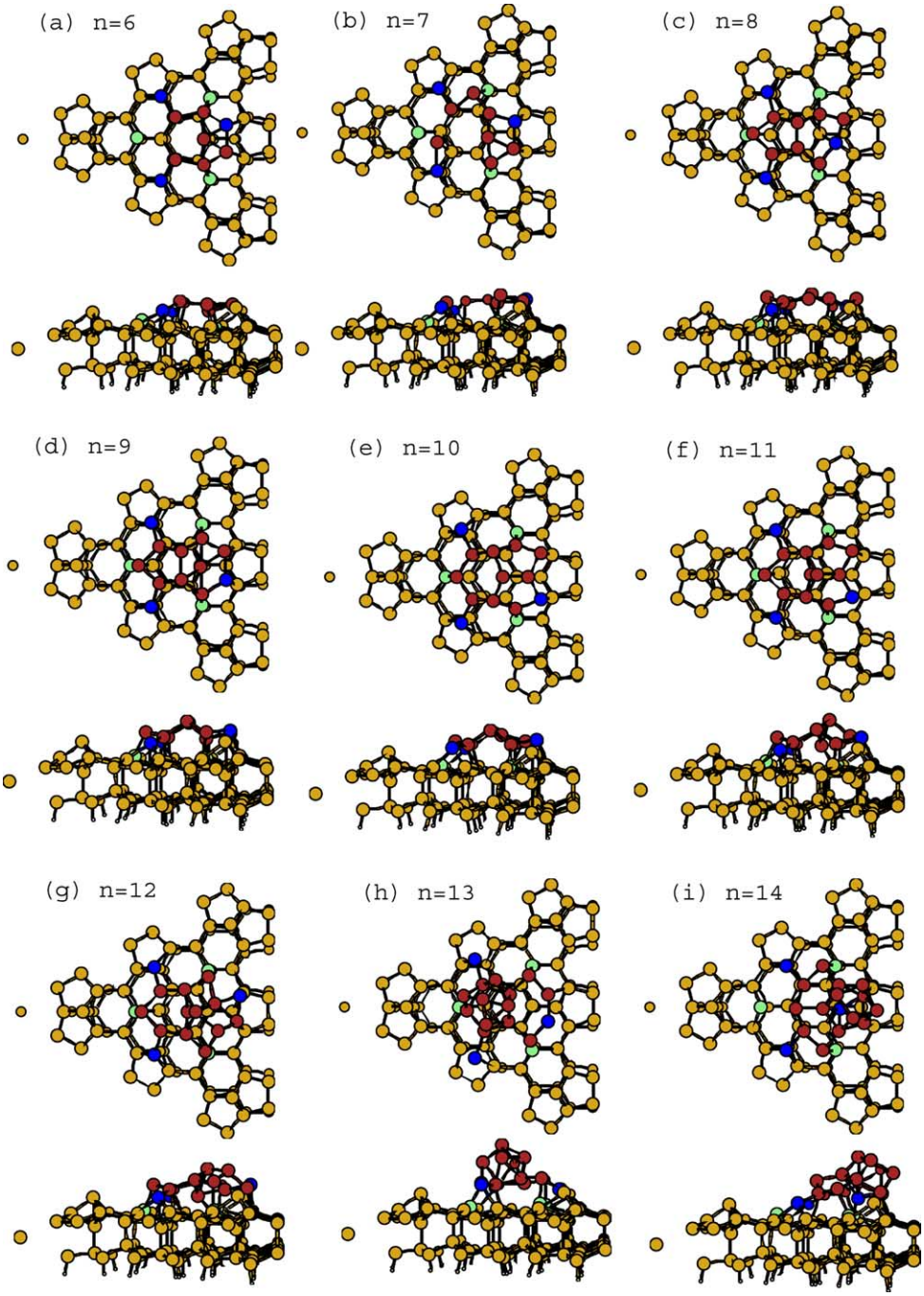


Fig. 2. The geometries of clusters with sizes ranging from $n = 6$ to 14 obtained by our genetic algorithm. The Si atoms in the cluster are colored red, while the three adatoms and the three rest atoms in the substrate that are involved in mating process are colored blue and green, respectively. The geometries shown are optimized with a full $7 \times 7$ unit cell. For clarity, only the faulted half of the Si(1 1 1) $7 \times 7$ surface is shown in the figure.

SURFACE SCIENCE LETTERS

bonds between one of the substrate adatoms and the corresponding three back-bond atoms are broken and the adatom is bonded with the deposited atoms. Another noteworthy feature is that for $n < 12$ the cluster exhibits a nearly planar geometry on the surface, whereas for $n \geqslant 13$ the cluster starts to show a three-dimensional growth.

In order to determine the size $n$ of the magic cluster observed in experiments and to study the relative stability of different sizes of Si clusters on the Si(1 1 1) surface, we calculated the surface energy per cluster atom $E_s$ as follows:

$$E_s = \frac{E - E_{sub} - nE_{bulk}}{n}, \quad (1)$$

where $E$ is the total energy of the cluster on the Si(1 1 1) $7 \times 7$ substrate, $E_{sub}$ is the energy of the Si(1 1 1) $7 \times 7$ substrate, and $E_{bulk}$ is the energy of bulk Si (per atom) in crystalline diamond structure. We first checked the surface energy ordering of different-sized clusters on the surface using tight-binding calculations. We found that the energy ordering is the same regardless the choice of substrate, i.e., half unit cell or the full $7 \times 7$ substrate, and the thickness of the substrate. This result indicates that the reduced Si substrate we used in our GA global search is sufficient for the present study. The plots of surface energies versus the size of the Si cluster obtained from the tight-binding calculation and first-principles calculations are shown in Fig. 3(a) and (b), respectively. The plots show that Si cluster on the faulted half of the $7 \times 7$ substrate is energetically more favorable than that on the unfaulted half. This agrees with STM observations that statistically more magic clusters reside on the faulted half than on the unfaulted half of the Si(1 1 1) $7 \times 7$ surface. We found that there is a sharp dip in the surface energy at $n = 8$, which is the most stable Si cluster on Si(1 1 1) $7 \times 7$ among the sizes that we considered. By comparing Fig. 3(a) and (b), we found that our tight-binding Si potential can reproduce the overall trend of the surface energies versus size of the Si cluster.

Our calculations suggest that the magic Si cluster on Si(1 1 1) $7 \times 7$ surface should correspond to the $n = 8$ structure as shown in Fig. 2(c) (as well as Fig. 5). This structure is energetically most

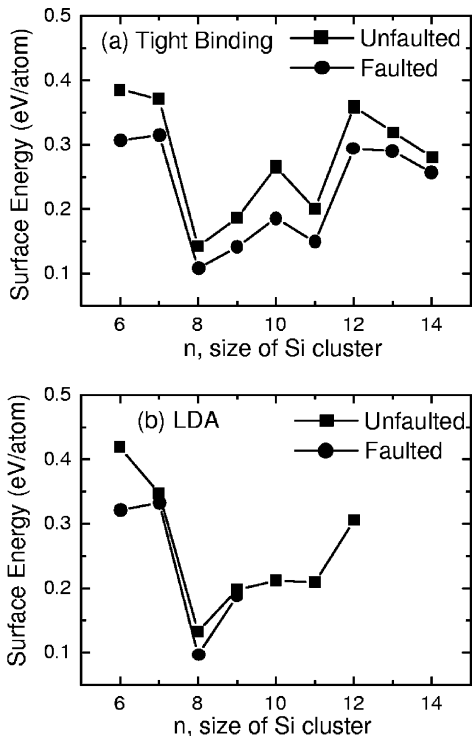


Fig. 3. The surface energy per cluster atom calculated by (a) tight-binding potential, and (b) by first-principles calculations. The curve with circles (square) corresponds to the Si cluster being placed on the faulted (unfaulted) half of the Si(1 1 1) $7 \times 7$ substrate.

favorable when compared with the other structures. The presence of this magic cluster ($n = 8$) minimizes its own dangling bonds while saturating that of the clean Si(1 1 1) $7 \times 7$ reconstruction surface, and does not introduce extra strained bonds or 5-fold Si coordination. We calculated simulated STM images using our atomic model of the Si magic cluster and compare it with experimental STM image. The simulated STM images are calculated according to the theory of Tersoff and Hamann [14] by tracing the height profile of constant tunneling current to produce a three-dimensional surface, which is then projected onto the $xy$-plane to produce our simulated STM images. As a benchmark, the simulated STM image for a clean Si(1 1 1) $(7 \times 7)$ reconstruction surface is shown in Fig. 4 in comparison with the experimental image [15]. In addition to the bright spots

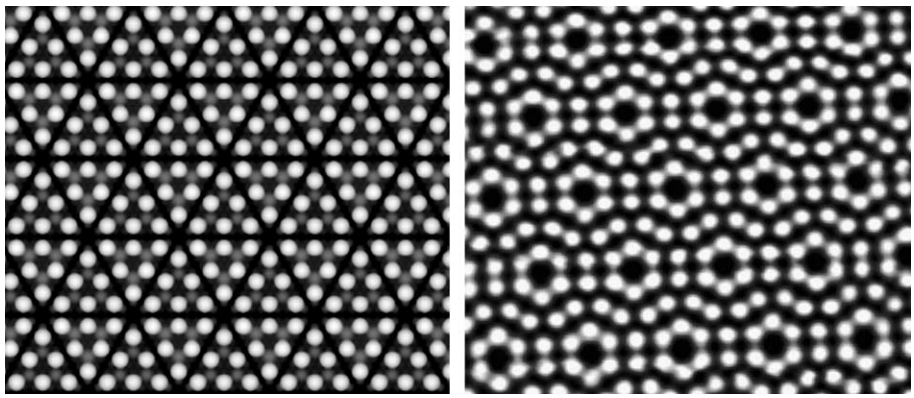

Fig. 4. Left: the simulated STM image of the Si(1 1 1) $7\times7$ at a bias of +1 V. Right: the experimental STM image of the Si(1 1 1) $7\times7$ at a bias of +1.5 V [15].

corresponding to the adatom positions (12 per $7\times7$ unit cell) as seen in the experiment, our simulated STM image also exhibits dimmer spots at the rest atom positions due to the higher resolution in the theoretical calculation. Our stimulated image for the clean $7\times7$ surface is also in a good agreement with other studies [16]. Next, our calculated empty state images with a bias of +1 V for silicon clusters on Si(1 1 1) ($7\times7$) surface with the cluster size $n=8$ and 9 are shown in Fig. 5 together with the experimental STM images reproduced from Ref. [1]. Both simulated empty state images show a ring-like feature. Within the ring, one circular bright spots and two elongated spots can be found for $n=8$, while there are six bright spots for $n=9$. Experimental STM images are shown in Fig. 5 as well for comparison. The experimental image on the left shows three spots, whereas the other STM image shows six equally bright spots. The difference between the two experimental images was attributed to tip effects. We note that our lowest energy $n=8$ structure has actually two degenerate states, one is shown in Fig. 5, and the other is the mirror image of the first one along the $[1\,1\,\bar{2}]$ direction. We have done TBMD simulation of our $n=8$ structure at elevated temperature, we found that there can be flipping between the two degenerate $n=8$ states. Due to the time-averaging of the two states, the experimental STM image would have a total of six spots instead of three as shown in the lower-right corner of Fig. 5. However, there may be interactions between the STM tip and the magic cluster such that one of the degenerate geometry is pinned, and hence the experiments can also observe three spots instead of six for certain STM tips as shown in the lower-left corner of Fig. 5. Apart from the ring, both our simulated images show three additional spots due to the three unsaturated atoms of the Si clusters, which are not observed in STM experiments [1].

In summary, we have performed global structural optimization using genetic algorithm to search for the ground state structures of Si clusters on the Si(1 1 1) $7\times7$ surface for $n=6$ up to 14. We found that Si clusters prefer to reside on the faulted half of the $7\times7$ substrate for all the sizes studied. When the Si cluster contains 13 atoms or more, it begins to exhibit three-dimensional growth. Placing six Si atoms according to the experimental bright spot positions does not produce a stable structure. Instead, our study suggests that the structure with $n=8$ as shown in Fig. 2(c) (as well as Fig. 5) could be the magic cluster observed in STM experiments [1].

## Acknowledgments

Ames Laboratory is operated for the US Department of Energy by Iowa State University under Contract No. W-7405-Eng-82. This work

SURFACE SCIENCE LETTERS

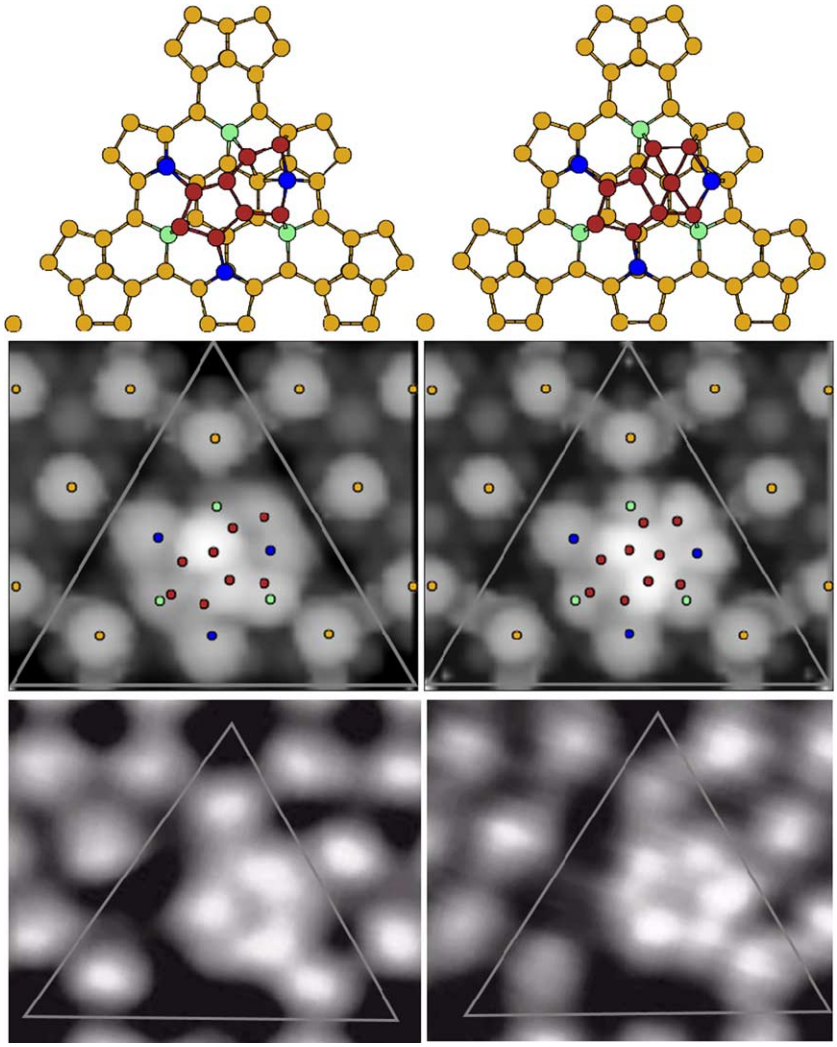

Fig. 5. Top: the positions of the cluster atoms for $n = 8$ (left) and $n = 9$ (right), the adatoms, and rest atoms on the Si(1 1 1) $7 \times 7$ are indicated and are colored in the same way as that in Fig. 2. Center: the simulated STM images of the $n = 8$ Si cluster (left) and $n = 9$ Si cluster (right) with a bias of +1 V. Bottom: the experimental STM images of two clusters taken at the sample biases of +1.8 V (left) and +1.2 V (right) with two different tips are reproduced from Ref. [1].

was supported by the Director for Energy Research, Office of Basic Energy Sciences including a grant of computer time at the National Energy Research Supercomputing Center (NERSC) in Berkeley and CCS at Oak Ridge National Laboratory. We thank Myron Hupalo in Ames Laboratory for supplying the experimental STM image of a clean Si (7×7) reconstruction surface.

## References

[1] I.S. Hwang, M.S. Ho, T.T. Tsong, Phys. Rev. Lett. 83 (1999) 120;
M.S. Ho, I.S. Hwang, T.T. Tsong, Phys. Rev. Lett. 84 (2000) 5792;
I.S. Hwang, M.S. Ho, T.T. Tsong, Surf. Sci. 514 (2002) 309;
M.S. Ho, I.S. Hwang, T.T. Tsong, Surf. Sci. 564 (2004) 93.

[2] V.G. Kotlyar, A.V. Zotov, A.A. Saranin, T.V. Kasyanova, M.A. Cherevik, I.V. Pisarenko, V.G. Lifshits, Phys. Rev. B 66 (2002) 165401.
[3] J.-F. Jia, X. Liu, J.-Z. Wang, J.-L. Li, X.S. Wang, Q.-K. Xue, Z.-Q. Li, Z. Zhang, S.B. Zhang, Phys. Rev. B 66 (2002) 165412.
[4] H.H. Chang, M.Y. Lai, J.H. Wei, C.M. Wei, Y.L. Wang, Phys. Rev. Lett. 92 (2004) 066103.
[5] C.Z. Wang, B.C. Pan, K.M. Ho, J. Phys.: Condens. Matter 11 (1999) 2043.
[6] D.M. Deaven, K.M. Ho, Phys. Rev. Lett. 75 (1995) 288.
[7] K.M. Ho, A.A. Shvartsburg, B. Pan, Z.Y. Lu, C.Z. Wang, J.G. Wacker, J.L. Eye, M.F. Jarrold, Nature (London) 392 (1998) 582.
[8] F.C. Chuang, C.V. Ciobanu, V.B. Shenoy, C.Z. Wang, K.M. Ho, Surf. Sci. 573 (2004) L375.
[9] F.C. Chuang, C.V. Ciobanu, C. Predescu, C.Z. Wang, K.M. Ho, Surf. Sci. 578 (2005) 183;
F.C. Chuang, C.V. Ciobanu, C.Z. Wang, K.M. Ho, J. Appl. Phys. 98 (2005) 073507.
[10] S. Baroni, A. Dal Corso, S. de Gironcoli, P. Giannozzi. Available from: <http://www.pwscf.org>.
[11] Hohenberg, W. Kohn, Phys. Rev. 136 (1964) B864;
W. Kohn, L.J. Sham, Phys. Rev. 140 (1965) A1135.
[12] D.M. Ceperley, B.J. Alder, Phys. Rev. Lett. 45 (1980) 566.
[13] J.P. Perdew, A. Zunger, Phys. Rev. B 23 (1981) 5048.
[14] J. Tersoff, D.R. Hamann, Phys. Rev. B 31 (1985) 805.
[15] The experimental STM image of Si(111) $7\times7$ is from M. Hupalo, private communications.
[16] K.D. Brommer, M. Needels, B.E. Larson, J.D. Joannopoulos, Phys. Rev. Lett. 68 (1992) 1355;
H. Lim, K. Cho, R.B. Capaz, J.D. Joannopoulos, K.D. Brommer, B.E. Larson, Phys. Rev. B 53 (1996) 15421;
Y.L. Wang, H.-J. Gao, H.M. Guo, H.W. Liu, I.G. Batyrev, W.E. McMahon, S.B. Zhang, Phys. Rev. B 70 (2004) 073312.